



Research article

Two methods based on second-order dynamical systems for solving a special class of nonlinear optimization problems

Juhe Sun¹, Guolin Huang^{1,*}, Li Wang¹ and Ning Ma²

¹ School of Science, Shenyang Aerospace University, Shenyang 110136, China

² School of Mechatronics Engineering, Shenyang Aerospace University, Shenyang 110136, China

* **Correspondence:** Email: 15023912554@163.com.

Abstract: Symbolic functions, as an important class of nonsmooth functions, play a key role in many fields such as system control and optimization theory. In this study, the special case of nonlinear optimization problems with sign function constraints is discussed in depth. Based on the smooth approximation theory, the study first adopts an approximate substitution method to smooth the nonsmooth constraints and then transforms them into differentiable optimization problems, thus effectively avoiding the numerical computational difficulties caused by the sign function. Second, the constrained optimization problem is transformed into an unconstrained optimization problem by constructing an exact penalty function. Third, two forms of second-order dynamical systems are established to solve the problem, and a rigorous theoretical analysis of the stability of these systems is conducted. Finally, the convergence and computational efficiency of the proposed method are verified by numerical simulation experiments of the system, and the simulation results fully prove the effectiveness and practicality of the algorithm.

Keywords: symbolic functions; nonlinear optimization problems; smooth approximation; penalty function method; second-order dynamical systems

1. Introduction

Nonlinear optimization problems incorporating discontinuous constraints are extensively employed across a multitude of disciplines, encompassing engineering design and economic management, among others. Notable instances of such problems involve optimization scenarios with setup costs or impulse control mechanisms, control issues pertaining to discrete-event systems [1–3], and state-control problems characterized by the discontinuous evolution of system parameters. Given the widespread application of these problems, conducting in-depth research on the solution methodologies for discontinuous optimization problems holds substantial significance. At present,

many types of discontinuous optimization problems have been developed, and this study focuses on the special class of optimization problems whose constraints contain “sign” functions. However, owing to the mathematical intricacies stemming from their discontinuous characteristics, the resolution of such problems is confronted with formidable theoretical and computational hurdles. To overcome this challenge, the study documented in [4] delved into the optimization problem characterized by constraint functions that incorporate jump discontinuities. It revealed that employing continuous extension methods alongside the introduction of auxiliary variables can be an effective strategy. These approaches facilitate the construction of an equivalent mixed-integer optimization model, which serves as a viable solution pathway for the given problem.

In optimization theory research, the solution of smooth optimization problems has obvious computational advantages compared with discontinuous optimization problems, and this consensus provides important methodological insights for dealing with discontinuous optimization problems. Based on this theoretical knowledge, researchers have proposed the innovative idea of using smooth functions to approximate discontinuous functions. The theoretical roots of this approach can be traced back to the groundbreaking work presented in [5]. This foundational study systematically delved into the treatment strategies for optimizing discontinuous functions and, for the first time, proposed a solution paradigm grounded in smoothing techniques. Building upon this foundation, the authors of [6] further advanced this research trajectory by offering a rigorous mathematical analysis of the optimality conditions pertinent to discontinuous constrained optimization problems, thereby reinforcing and expanding the theoretical framework established by its predecessor. As research progresses in depth, scholars have gradually refined the approximation technique centered around the average function within the realm of optimization theory. This method has undergone systematic theoretical elaboration and algorithmic realization, as detailed in the existing literature [7–9]. It serves as a potent numerical computational instrument for addressing discontinuous optimization problems. Furthermore [10–12] provide applications of averaging functions to nonlinear and semifinite programming.

Drawing inspiration from the pioneering research conducted by Cui et al. [13], this study, based on smooth approximation theory, puts forward two optimization methods to tackle a specific class of nonlinear optimization problems. Given the prominent discontinuity characteristic of the sign function within the constraints, this paper first proposes a novel technical approach to handle the sign function. This handling process is achieved by constructing a smooth approximation function, thereby effectively overcoming the numerical computational challenges posed by the sign function and further reformulating the original discontinuous constrained optimization problem into an equivalent continuous and differentiable optimization model. Second, during the solution process, this study draws on the theoretical foundations presented in the existing literature [14–16]. By introducing parameters, it employs the exact penalty function method to transform the reformulated differentiable constrained optimization problem into an unconstrained optimization form. Third, building upon previous research that utilized first-order dynamical systems to solve continuous optimization problems [17], this study innovatively devises two distinct forms of second-order dynamical systems and provides rigorous stability proofs for each form. Ultimately, numerical case studies are simulated and analyzed individually to substantiate the superior performance of the proposed algorithms in terms of convergence properties and computational efficiency.

This study is organized as follows: Section 2 offers a systematic exposition of the fundamental

concepts of relevant knowledge and the modeling of optimization problems; Section 3 delves into an in-depth discussion on the implementation process of the smooth approximation method; Section 4 constructs the first form of the second-order dynamical system and analyzes its stability; Section 5 builds the second form of the second-order dynamical system and gives a rigorous proof of global convergence; Section 6 provides a theoretical comparison between second-order dynamical system approaches and first-order dynamical system approaches; Section 7 verifies the performance of the algorithm through numerical simulation experiments. Finally, the paper concludes with a summary of the key findings and an outlook on future research directions.

2. Model for the optimization problem of the symbolic function

Definition 2.1 The sign function $sgn(x)$ is defined as

$$sgn(x) = \begin{cases} 1, & x \in (0, +\infty), \\ 0, & x = 0, \\ -1, & x \in (-\infty, 0). \end{cases} \quad (2.1)$$

The graph of the symbolic function defined above is shown in Figure 1:

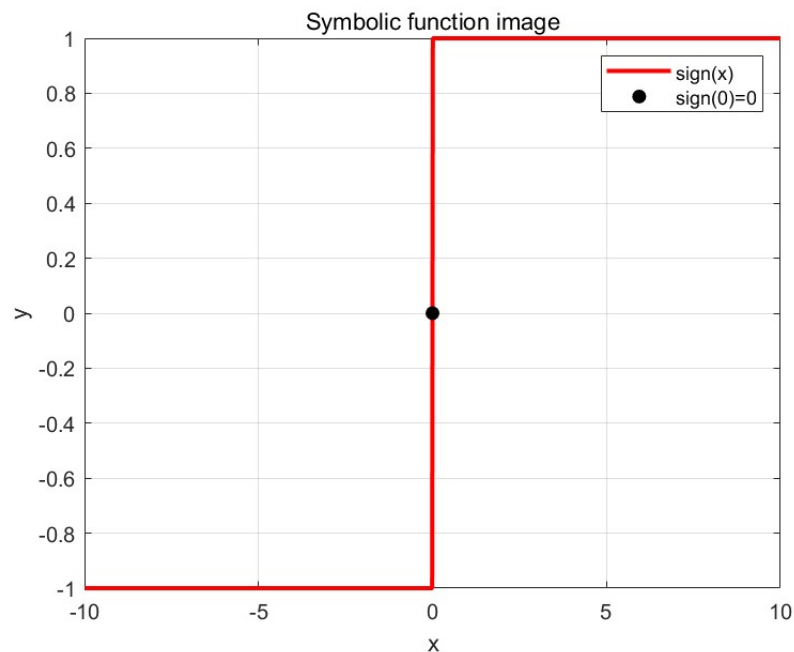


Figure 1. Symbolic function image.

Definition 2.2 Penalty function method

In practical problems, most optimization problems involve constraints, and an effective way to deal with constraints is the penalty function method. The basic principle of the penalty function method is

given below, and the mathematical model of the optimization problem with constraints is as follows:

$$\begin{aligned} \min f(x) \\ \text{s.t. } g_i(x) \leq 0, i = 1, \dots, n, \\ h_j(x) = 0, j = 1, \dots, m, \end{aligned} \quad (2.2)$$

where $f(x)$, $g_i(x)$, and $h_j(x)$ are continuous functions on $x \in R^n$.

The penalty function method to transform the constrained optimization problem comprises the following basic process: the constrained optimization problem is converted into an unconstrained optimization problem, and the resulting sequence of optimal solutions will gradually approximate the optimal solution of the original problem. The constructed penalty function can be expressed in the following form:

$$\min F(x, r_k) = f(x) + r_k P(x), \quad (2.3)$$

where $P(x) = \sum_{i=1}^n \vartheta(g_i(x)) + \sum_{j=1}^m \varphi(h_j(x))$, $\vartheta = \max(0, g_i(x))^2$, $\varphi = |h_j(x)|^2$, r_k is the penalty factor.

Definition 2.3 Model of the optimization problem with sign function constraints

In this paper, we consider the following class of nonsmooth constrained optimization problems:

$$\begin{aligned} \min f(x) \\ \theta_i(x) \operatorname{sgn}(k_i(x)) \leq b, i = 1, \dots, n, \\ h_j(x) = a, j = 1, \dots, m, \end{aligned} \quad (2.4)$$

where $\operatorname{sgn}(\bullet)$ denotes the sign function; see Definition 2.1 for details.

Obviously, the constraints increase the complexity of the problem, and assuming that this symbolic function does not exist, the analysis of the problem will be relatively simple. So, a new idea arises to replace the symbolic function with a smooth approximation, thus overcoming the discontinuity of the symbolic function and further simplifying the problem.

3. Smooth approximation of constraints

Definition 3.1 Let $\psi : R^2 \rightarrow R$ be a real-valued function and satisfy the following two conditions:

- 1) Function $\psi(x, a)$ is a smooth function, where a is an argument;
- 2) $\lim_{a \rightarrow +\infty} \psi(x, a) = \operatorname{sgn}(x)$.

Then, the function $\psi(x, a)$ is said to be a smooth approximation to the symbolic function $\operatorname{sgn}(x)$.

Proposition 3.2 When $a > 0$, assume that the function $\psi(x, a)$ has the following properties:

- A. When $x > 0$, $\psi(x, a)$ is monotonically increasing with respect to a , and $\psi(x, a)$ is monotonically decreasing with respect to a when $x < 0$;
- B. $\psi(x, a)$ is monotonically increasing about x ;
- C. $\psi(x, a)$ is higher-order differentiable about x ;
- D. For any $x \in R$, $\psi(x, a) \in [-1, 1]$, and $\psi(0, a) = 0$, $\lim_{a \rightarrow +\infty} \psi(x, a) = \operatorname{sgn}(x)$.

In this paper, consider the function $\psi(x, a) = ax / \sqrt{1 + a^2 x^2}$, where $a > 0$. Next, verify that $\psi(x, a)$ satisfies Proposition 3.2.

Proof. The partial derivatives of $\psi(x, a) = ax / \sqrt{1 + a^2 x^2}$ with respect to a are first calculated

as follows:

$$\frac{\partial\psi}{\partial a} = \frac{x(1 + a^2x^2) - a^2x^3}{(1 + a^2x^2)^{\frac{3}{2}}} = \frac{x}{(1 + a^2x^2)^{\frac{3}{2}}}.$$

When $x > 0$, $\partial\psi/\partial a > 0$, $\psi(x, a)$ monotonically increases with respect to a ; when $x < 0$, $\partial\psi/\partial a < 0$, $\psi(x, a)$ monotonically decreases with respect to a , so Property A holds.

Next, calculate the partial derivative of $\psi(x, a) = ax/\sqrt{1 + a^2x^2}$ with respect to x :

$$\frac{\partial\psi}{\partial x} = \frac{a(1 + a^2x^2) - a^3x^2}{(1 + a^2x^2)^{\frac{3}{2}}} = \frac{a}{(1 + a^2x^2)^{\frac{3}{2}}}.$$

Because $a > 0$, and therefore $\partial\psi/\partial x > 0$, $\psi(x, a)$ is monotonically increasing with respect to x . Therefore Property B holds.

Because functions $T_1(x, a) = ax$ and $T_2(x, a) = 1 + a^2x^2$ are higher-order differentiable for any x , and $\psi(x, a)$ is composed of $T_1(x, a)$ and $T_2(x, a)$ by division, $\psi(x, a)$ is higher-order differentiable with respect to x ; thus, Property C holds.

Because $\lim_{x \rightarrow -\infty} \psi(x, a) = -1$, $\lim_{x \rightarrow +\infty} \psi(x, a) = 1$, and $\psi(x, a)$ is monotonically increasing with respect to x , for any $x \in \mathbb{R}$, $\psi(x, a) \in [-1, 1]$, $\psi(x, a) = 0$ holds if and only if $x = 0$.

When $x > 0$, $\lim_{a \rightarrow +\infty} \psi(x, a) = 1$; when $x < 0$, $\lim_{a \rightarrow +\infty} \psi(x, a) = -1$; and when $x = 0$, $\lim_{a \rightarrow +\infty} \psi(x, a) = 0$, so $\lim_{a \rightarrow +\infty} \psi(x, a) = \text{sgn}(x)$ holds. □

To summarize, for $x \in \mathbb{R}$, the function $\psi(x, a) = ax/\sqrt{1 + a^2x^2}$ is a smooth approximation of the symbolic function $\text{sgn}(x)$.

Figure 2 shows the image of the smooth approximation of the symbolic function $\text{sgn}(x)$ by $\psi(x, a) = ax/\sqrt{1 + a^2x^2}$ at different parameters a .

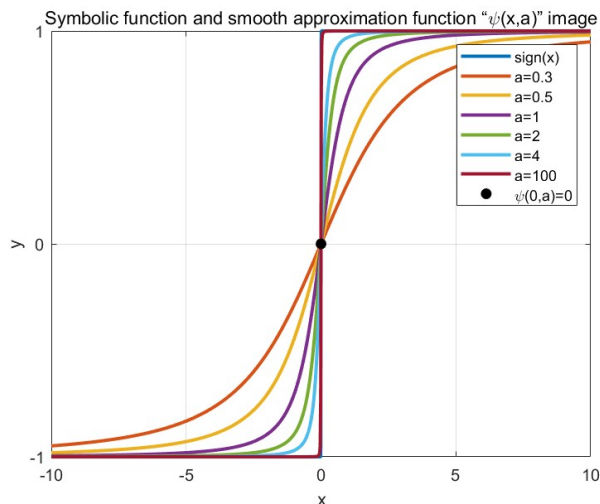


Figure 2. $\psi(x, a)$ smooth approximate curves with different parameters a .

It is noteworthy that although it can be clearly observed from the relevant charts that as the value of parameter a continuously increases, the adopted smoothing approximation method demonstrates extremely favorable results. Specifically, during the process of parameter a increasing, the degree of

fit between the smoothing approximation curve and the real curve gradually improves, and the error range continuously narrows. However, it is essential to recognize that this smoothing approximation method, constructed based on specific conditions and models, may exhibit the following limitations:

- 1) The accuracy of the smoothed approximation may exhibit certain precision errors relative to the original problem;
- 2) The smoothing approximation may affect the optimal solution of the original optimization problem.

Although smooth approximation may have certain limitations, it offers us a new approach to handling symbolic functions. Thus, we can obtain a smooth approximate constrained optimization problem for the discontinuous optimization problem (2.4) as follows:

$$\begin{aligned} \min f(x) \\ \text{s.t. } \theta_i(x)\psi(k_i(x), a) \leq b, i = 1, \dots, n, \\ m_j(x) = a, j = 1, \dots, m, \end{aligned} \quad (3.1)$$

where $\psi(k_i(x), a) = ak_i(x) / \sqrt{1 + a^2k_i(x)^2}$.

4. The first form second-order dynamical system

Next, the above smooth constrained optimization problem (3.1) using the penalty function method can be written as the following unconstrained optimization problem:

$$\min \Phi(x) = f(x) + r_k \left(\sum_{i=1}^n \vartheta(g_i(x)) + \sum_{j=1}^m \varphi(h_j(x)) \right), \quad (4.1)$$

where $\vartheta(g_i(x)) = \{\max(0, g_i(x))\}^2$, $\varphi(h_j(x)) = |h_j(x)|^2$, $g_i(x) = \theta_i(x)\psi(k_i(x), a) - b$, and $h_j(x) = m_j(x) - a$.

In previous studies, methods for solving the unconstrained optimization problem (4.1) include Sun et al. [17] giving a first-order dynamical system with the following dynamical system model:

$$\begin{cases} \frac{d(x(t))}{dt} = -\rho \nabla \Phi(x(t)), \\ x(t_0) = x_0, \end{cases} \quad (4.2)$$

where $\rho > 0$ is a scaling factor.

In order to solve the above unconstrained optimization problem, we build a second-order dynamical system (4.3) of the first form to solve the above unconstrained optimization problem, inspired by the studies in literature [18, 19]:

$$\ddot{x}(t) + \gamma(t)\dot{x}(t) + \beta(t)\nabla\Phi(x(t)) = 0, \quad (4.3)$$

where $\gamma(t) = \alpha/t$ is the positive viscous damping coefficient, and $\beta(t)$ is the time-scale coefficient.

Next, we analyze the convergence of the trajectories of the damped gradient dynamical system (4.3).

In the case of $\Phi(x) \equiv 0$, the dynamical system (4.3) is transformed into the following form:

$$\ddot{x}(t) + \gamma(t)\dot{x}(t) = 0. \quad (4.4)$$

Multiplying both sides of the system (4.4) by the integrating factor $p(t) = e^{\int_{t_0}^t \gamma(u)du}$, we have

$$p(t)\ddot{x}(t) + p(t)\gamma(t)\dot{x}(t) = 0. \quad (4.5)$$

Integrating the system (4.5) over the interval $[t_0, t]$, we have that

$$p(t)\dot{x}(t) = A. \quad (4.6)$$

Bringing $t = t_0$ into Eq (4.6) gives $A = \dot{x}(t_0)$. Thus, the above equation (4.6) can be further written as

$$\dot{x}(t) = \frac{\dot{x}(t_0)}{p(t)}. \quad (4.7)$$

Integrating Eq (4.6), we obtain

$$x(t) = x(t_0) + \dot{x}(t_0) \int_{t_0}^t \frac{1}{p(u)} du. \quad (4.8)$$

It can be seen from above that the trajectory $x(t)$ converges if and only $\dot{x}(t_0) = 0$ or

$$(H_0) : \int_{t_0}^{+\infty} \frac{1}{p(u)} du < \infty.$$

Indeed, this condition is identified as necessary for the convergence of the trajectories when Φ is a convex function with a continuous minimum; see [20, 21].

So, the following assumes that the condition

$$(H)_0 : \int_{t_0}^{+\infty} \frac{1}{p(u)} du < +\infty$$

holds, for the choice $\gamma(t) = \alpha/t$; this condition can be derived explicitly. Further, the function $\Gamma(t)$ is formulated as follows:

$$\Gamma(t) = p(t) \int_t^{+\infty} \frac{1}{p(u)} du. \quad (4.9)$$

Derivation of the Eq (4.9) yields

$$\dot{\Gamma}(t) = \gamma(t)\Gamma(t) - 1. \quad (4.10)$$

In addition, the global energy function $W(t)$ and the anchor function $h(t)$ are defined as follows, respectively:

$$W(t) = \frac{1}{2} \|\dot{x}(t)\|^2 + \beta(t)(\Phi(x(t)) - \min_{\mathcal{H}} \Phi), \quad (4.11)$$

and

$$h(t) = \frac{1}{2} \|x(t) - x^*\|^2, \quad (4.12)$$

where $x^* \in \operatorname{argmin} \Phi$; the solution set $\operatorname{argmin} \Phi$ is nonempty. The Lyapunov analytic function $\xi(t)$, which plays a key role in the convergence analysis of damped gradient systems, is given next and is mathematically defined as follows:

$$\xi(t) = \Gamma(t)^2 W(t) + h(t) + \Gamma(t)\dot{h}(t). \quad (4.13)$$

Combining the definitions of the above several functions and substituting the mathematical expressions for $h(t)$ and $W(t)$ into the function $\xi(t)$, the following equation can be obtained:

$$\xi(t) = \Gamma(t)^2 \beta(t)(\Phi(x(t)) - \min_{\mathcal{H}} \Phi) + \frac{1}{2} \|x(t) - x^* + \Gamma(t)\dot{x}(t)\|^2. \quad (4.14)$$

Because $\beta(t) \geq 0$, and $\Phi(x(t)) - \min \Phi \geq 0$, there is $\xi(t) \geq 0$. Therefore, $\xi(t)$ is a nonnegative function.

Now, assume $\xi(t) = \xi_1(t) + \xi_2(t)$, where $\xi_1(t) = \Gamma(t)^2 \beta(t) (\Phi(x(t)) - \min \Phi)$, $\xi_2(t) = \frac{1}{2} \|x(t) - x^* + \Gamma(t)\dot{x}(t)\|^2$.

Theorem 4.1 Let $\Phi : \mathcal{H} \rightarrow R$ be a convex function with nonempty solution set $\text{argmin } \Phi$, where \mathcal{H} is a Hilbert space. The positive viscous damping coefficients $\gamma(t)$ and the time scale coefficients $\beta(t)$ are both continuous functions in $t \in [t_0, +\infty)$ whose growth conditions $(H)_{\gamma, \beta}$ are expressed as follows:

$$\Gamma(t)\dot{\beta}(t) \leq \beta(t)(3 - 2\gamma(t)\Gamma(t)). \quad (4.15)$$

Therefore, the trajectories $x(t)$ and $\Gamma(t)\dot{x}(t)$ of the dynamical system are bounded on $t \in [t_0, +\infty)$, and the rate of convergence is when $t \rightarrow +\infty$:

$$\Phi(x(t)) - \min_{\mathcal{H}} \Phi = O\left(\frac{1}{\beta(t)\Gamma(t)^2}\right). \quad (4.16)$$

Proof First, the derivation of $\xi(t)$ is performed so that we have

$$\dot{\xi}(t) = \dot{\xi}_1(t) + \dot{\xi}_2(t), \quad (4.17)$$

where $\dot{\xi}_1(t)$ is formulated as follows:

$$\dot{\xi}_1(t) = (\dot{\beta}(t)\Gamma(t)^2 + 2\beta(t)\dot{\Gamma}(t)\Gamma(t))(\Phi(x(t)) - \min_{\mathcal{H}} \Phi) + \beta(t)\Gamma(t)^2 \langle \nabla \Phi(x(t)), \dot{x}(t) \rangle,$$

and $\dot{\xi}_2(t)$ is expressed as follows:

$$\dot{\xi}_2(t) = \langle \dot{x}(t) + \dot{\Gamma}(t)\dot{x}(t) + \Gamma(t)\ddot{x}(t), x(t) - x^* + \Gamma(t)\dot{x}(t) \rangle.$$

Bringing $\dot{\Gamma}(t) = \gamma(t)\Gamma(t) - 1$ into $\dot{\xi}_2(t)$, we have

$$\dot{\xi}_2(t) = \langle \gamma(t)\dot{x}(t)\Gamma(t) + \Gamma(t)\ddot{x}(t), x(t) - x^* + \Gamma(t)\dot{x}(t) \rangle. \quad (4.18)$$

Based on the established dynamical system (4.3), Eq (4.18) can be further transformed into the following Eq (4.19):

$$\dot{\xi}_2(t) = \langle -\beta(t)\nabla \Phi(x(t))\Gamma(t), x(t) - x^* + \Gamma(t)\dot{x}(t) \rangle. \quad (4.19)$$

Bringing $\dot{\xi}_1(t)$ and $\dot{\xi}_2(t)$ into Eq (4.17), we get

$$\dot{\xi}(t) = (\dot{\beta}(t)\Gamma(t)^2 + 2\beta(t)\dot{\Gamma}(t)\Gamma(t))(\Phi(x(t)) - \min_{\mathcal{H}} \Phi) - \beta(t)\Gamma(t) \langle \nabla \Phi(x(t)), x(t) - x^* \rangle.$$

Also, because the function Φ is convex, it is deduced that the following inequality holds:

$$\dot{\xi}(t) \leq \Gamma(t)(\dot{\beta}(t)\Gamma(t) + 2\beta(t)\dot{\Gamma}(t) - \beta(t))(\Phi(x(t)) - \min_{\mathcal{H}} \Phi). \quad (4.20)$$

Bringing $\dot{\Gamma}(t) = \gamma(t)\Gamma(t) - 1$ into (4.20), we have

$$\dot{\xi}(t) \leq \Gamma(t)(\dot{\beta}(t)\Gamma(t) + \beta(t)(2\gamma(t)\Gamma(t) - 3))(\Phi(x(t)) - \min_{\mathcal{H}} \Phi). \quad (4.21)$$

Because of the growth condition $(H)_{\gamma,\beta} : \Gamma(t)\dot{\beta}(t) \leq \beta(t)(3 - \gamma(t)\Gamma(t))$, there is $\dot{\xi}(t) \leq 0$ as $\xi(t)$ is nonincreasing. When this result is further combined with $\xi(t) \geq 0$, it can be deduced that $\xi(t)$ is bounded. From the above definition of the function $\xi(t)$, it follows that its fundamental component $\|x(t) - x^* + \Gamma(t)\dot{x}(t)\|^2$ is also bounded, and there is

$$\frac{1}{2}(\|x(t) - x^*\|^2 + 2\Gamma(t) \langle x(t) - x^*, \dot{x}(t) \rangle) \leq \xi(t_0). \quad (4.22)$$

Combined with the above definition of the anchor function $h(t)$, it follows that

$$\dot{h}(t) = \langle x(t) - x^*, \dot{x}(t) \rangle. \quad (4.23)$$

Bringing $h(t)$ and $\dot{h}(t)$ into (4.22), we have

$$h(t) + \Gamma(t)\dot{h}(t) \leq \xi(t_0). \quad (4.24)$$

Suppose

$$f(t) = \int_t^{+\infty} \frac{1}{p(u)} du.$$

Because

$$(H)_0 : \int_{t_0}^{+\infty} \frac{1}{p(u)} du < +\infty,$$

the function $f(t)$ is bounded when $t_0 \leq t$.

Divide both sides of Eq (4.21) simultaneously by $p(t)$, so that

$$\frac{h(t)}{p(t)} + \frac{\Gamma(t)}{p(t)}\dot{h}(t) \leq \frac{\xi(t_0)}{p(t)} \quad (4.25)$$

holds.

Because $\dot{f}(t) = -1/p(t)$ and $\Gamma(t) = p(t)f(t)$, Eq (4.25) can be equivalent to Eq (4.26):

$$-\dot{f}(t)h(t) + f(t)\dot{h}(t) \leq -\dot{f}(t)\xi(t_0). \quad (4.26)$$

Shifting the terms of Eq (4.26), we get

$$f(t)\dot{h}(t) - \dot{f}(t)(h(t) - \xi(t_0)) \leq 0. \quad (4.27)$$

It is further possible to introduce

$$\frac{d}{dt} \left(\frac{h(t) - \xi(t_0)}{f(t)} \right) = \frac{f(t)\dot{h}(t) - \dot{f}(t)(h(t) - \xi(t_0))}{f(t)^2} \leq 0. \quad (4.28)$$

Integrating the above Eq (4.28) yields that there exists K such that $h(t) \leq Kf(t) + \xi(t_0)$ so that the trajectory $x(t)$ of the solution to the dynamical system can be obtained to be bounded, and that $\Gamma(t)\dot{x}(t)$ is bounded on $t \in [t_0, +\infty)$.

It is known that the function $\xi(t)$ is bounded and on (t_0, t) , so there is $\xi(t) \leq \xi(t_0)$. Eventually, based on the definition of $\xi(t)$, for any $t \geq t_0$, there are

$$\Phi(x(t)) - \min_{\mathcal{H}} \Phi \leq \frac{\xi(t_0)}{\beta(t)\Gamma(t)^2}, \quad (4.29)$$

its equivalent in terms of

$$\Phi(x(t)) - \min_{\mathcal{H}} \Phi \leq O\left(\frac{1}{\beta(t)\Gamma(t)^2}\right). \quad (4.30)$$

Therefore, Theorem 4.1 holds. \square

5. The second form second-order dynamical system

In order to demonstrate whether external perturbations have any effect on solving the unconstrained optimization problem, a second form of the second-order dynamical system (5.1) will be built in this section to solve the above unconstrained optimization problem (4.1):

$$\ddot{x}(t) + \gamma(t)\dot{x}(t) + \beta(t)\nabla\Phi(x(t)) = g(t), \quad (5.1)$$

where $g(t) \neq 0$ but is sufficiently small.

The convergence of the second-order dynamical system (5.1) based on the external action is analyzed next.

Let $\Phi : \mathcal{H} \rightarrow R$ be a convex continuous differentiable function, where \mathcal{H} is a Hilbert space, and $\text{argmin } \Phi$ is nonempty. Take $\gamma(t), \beta(t)$ to be continuous functions and $\gamma(t)$ to satisfy the $(H)_0$ condition and $g(t)$ to be locally integrable.

Theorem 5.1 If condition $(H)_g : \int_{t_0}^{+\infty} \Gamma(t)\|g(t)\|dt < +\infty$ holds, then the following two statements hold for any solution $x \in \mathcal{H}$ belonging to the dynamical system (5.1):

1) Under condition $(H)_{\gamma,\beta} : \dot{\beta}(t)\Gamma(t) \leq \beta(t)(3 - 2\gamma(t)\Gamma(t))$, $x(t)$ and $\Gamma(t)\dot{x}(t)$ are bounded on $t \in [t_0, +\infty)$, and when $t \rightarrow +\infty$, the rate of convergence between the dynamical system and the optimization problem is as follows:

$$\Phi(x(t)) - \min_{\mathcal{H}} \Phi = O\left(\frac{1}{\beta(t)\Gamma(t)^2}\right). \quad (5.2)$$

2) Under condition $(H)_{\gamma,\beta}^+ : \dot{\beta}(t)\Gamma(t) \leq \beta(t)(3 - \rho - 2\gamma(t)\Gamma(t))$, the following conclusions hold:

$$\int_{t_0}^{+\infty} \beta(t)\Gamma(t)(\Phi(x(t)) - \min_{\mathcal{H}} \Phi)dt < +\infty. \quad (5.3)$$

Proof As a Lyapunov function, the same analytic function $\xi(t)$, which is defined when $t \geq t_0$, is used as in the previous section:

$$\xi(t) = \xi_1(t) + \xi_2(t), \quad (5.4)$$

where $\xi_1(t) = \beta(t)\Gamma(t)^2(\Phi(x(t)) - \min_{\mathcal{H}} \Phi)$, $\xi_2(t) = \frac{1}{2}\|x(t) - x^* + \Gamma(t)\dot{x}(t)\|^2$.

Derivation of $\xi(t)$ gives

$$\dot{\xi}(t) = \dot{\xi}_1(t) + \dot{\xi}_2(t), \quad (5.5)$$

where

$$\dot{\xi}_1(t) = \frac{d(\beta(t)\Gamma(t)^2)}{dt}(\Phi(x(t)) - \min_{\mathcal{H}} \Phi) + \beta(t)\Gamma(t)^2 \langle \nabla\Phi(x(t)), \dot{x}(t) \rangle,$$

and

$$\dot{\xi}_2(t) = \left\langle \frac{d(x(t) - x^* + \Gamma(t)\dot{x}(t))}{dt}, x(t) - x^* + \Gamma(t)\dot{x}(t) \right\rangle.$$

The dynamical system (5.1) is next shifted to first turn it into:

$$\ddot{x}(t) + \gamma(t)\dot{x}(t) = g(t) - \beta(t)\Phi(x(t)). \quad (5.6)$$

Eq (5.6) is then obtained by multiplying both sides of $\Gamma(t)$, simultaneously:

$$\ddot{x}(t)\Gamma(t) + \gamma(t)\dot{x}(t)\Gamma(t) = g(t)\Gamma(t) - \beta(t)\Phi(x(t))\Gamma(t). \quad (5.7)$$

By combining $\dot{\Gamma}(t) = \gamma(t)\Gamma(t) - 1$, Eq (5.7) can be equivalently transformed into the following Eq (5.8):

$$\ddot{x}(t)\Gamma(t) + \dot{x}(t)\dot{\Gamma}(t) + \dot{x}(t) = g(t)\Gamma(t) - \beta(t) \nabla \Phi(x(t))\Gamma(t). \quad (5.8)$$

Obviously, the above Eq (5.8) can be further expressed as:

$$\frac{d(x(t) - x^* + \dot{x}(t)\Gamma(t))}{dt} = g(t)\Gamma(t) - \beta(t)\Phi(x(t))\Gamma(t). \quad (5.9)$$

Bringing Eq (5.9) into Eq (5.5), it follows that

$$\begin{aligned} \dot{\xi}(t) &= \frac{d(\beta(t)\Gamma(t)^2)}{dt} (\Phi(x(t)) - \min_{\mathcal{H}} \Phi) + \beta(t)\Gamma(t)^2 \langle \nabla \Phi(x(t)), \dot{x}(t) \rangle \\ &\quad + \left\langle \frac{d(x(t) - x^* + \Gamma(t)\dot{x}(t))}{dt}, x(t) - x^* + \Gamma(t)\dot{x}(t) \right\rangle \\ &= \frac{d(\beta(t)\Gamma(t)^2)}{dt} (\Phi(x(t)) - \min_{\mathcal{H}} \Phi) + \langle g(t)\Gamma(t), x(t) - x^* + \Gamma(t)\dot{x}(t) \rangle \\ &\quad - \langle \beta(t) \nabla \Phi(x(t))\Gamma(t), x(t) - x^* \rangle \end{aligned} \quad (5.10)$$

Using the convexity of Φ , we have

$$\langle \nabla \Phi(x(t)), x(t) - x^* \rangle \geq \Phi(x(t)) - \Phi(x^*). \quad (5.11)$$

It is further possible to introduce

$$\dot{\xi}(t) \leq \left(\frac{d(\beta(t)\Gamma(t)^2)}{dt} - \beta(t)\Gamma(t) \right) (\Phi(x(t)) - \min_{\mathcal{H}} \Phi) + \Gamma(t) \|g(t)\| \|x(t) - x^* + \Gamma(t)\dot{x}(t)\|.$$

Combining $\dot{\Gamma}(t) = \gamma(t)\Gamma(t) - 1$ with $(H)_{\gamma,\beta} : \dot{\beta}(t)\Gamma(t) \leq \beta(t)(3 - 2\gamma(t)\Gamma(t))$ gives:

$$\begin{aligned} \frac{d(\beta(t)\Gamma(t)^2)}{dt} - \beta(t)\Gamma(t) &= \dot{\beta}(t)\Gamma(t)^2 + 2\beta(t)\Gamma(t)\dot{\Gamma}(t) - \beta(t)\Gamma(t) \\ &= \dot{\beta}(t)\Gamma(t)^2 + 2\beta(t)\Gamma(t)(\gamma(t)\Gamma(t) - 1) - \beta(t)\Gamma(t) \\ &= \dot{\beta}(t)\Gamma(t)^2 + \beta(t)\Gamma(t)(2\gamma(t)\Gamma(t) - 3) \\ &= \Gamma(t)(\dot{\beta}(t)\Gamma(t) + \beta(t)(2\gamma(t)\Gamma(t) - 3)) \\ &\leq 0 \end{aligned} \quad (5.12)$$

Thus, $\dot{\xi}(t) \leq \Gamma(t)\|g(t)\|\|x(t) - x^* + \Gamma(t)\dot{x}(t)\|$ holds. Because $\xi(t) = \beta(t)\Gamma(t)^2 + \frac{1}{2}\|x(t) - x^* + \Gamma(t)\dot{x}(t)\|$, it follows that

$$\dot{\xi}(t) \leq \Gamma(t)\|g(t)\|\|x(t) - x^* + \Gamma(t)\dot{x}(t)\| \leq \Gamma(t)\|g(t)\| \sqrt{2\xi(t)}. \quad (5.13)$$

By integrating the above Eq (5.13) and combining it with condition $(H)_g$, it can be derived that

$$\sqrt{\xi(t)} \leq \sqrt{\xi(t_0)} + \frac{1}{\sqrt{2}} \int_{t_0}^{+\infty} \Gamma(t)\|g(t)\| dt < \infty. \quad (5.14)$$

Therefore, the first conclusion in Theorem 5.1 holds.

Additionally, it follows that $\|x(t) - x^* + \Gamma(t)\dot{x}(t)\|^2$ is bounded, and so there is:

$$\|x(t) - x^*\| + 2\Gamma(t) \langle x(t) - x^*, \dot{x}(t) \rangle \leq C. \quad (5.15)$$

Letting

$$k(t) = \frac{1}{2}\|x(t) - x^*\|,$$

Eq (5.15) can be simplified to:

$$k(t) + \Gamma(t)\dot{k}(t) \leq \frac{1}{2}C. \quad (5.16)$$

It is clear to show that the trajectory $x(t)$ is bounded and that $\Gamma(t)\dot{x}(t)$ is also bounded.

Assuming $W = x(t) - x^* + \Gamma(t)\dot{x}(t) > 0$, we have

$$\dot{\xi}(t) \leq \left(\frac{d(\beta(t)\Gamma(t)^2)}{dt} - \beta(t)\Gamma(t) \right) (\Phi(x(t)) - \min_{\mathcal{H}} \Phi) + W \cdot \Gamma(t)\|g(t)\|. \quad (5.17)$$

Integrating Eq (5.17), it can be derived on the basis that condition $\dot{\beta}(t)\Gamma(t) \leq \beta(t)(3 - \rho - 2\gamma(t)\Gamma(t))$ holds:

$$\int_{t_0}^{+\infty} \beta(t)\Gamma(t) (\Phi(x(t)) - \min_{\mathcal{H}} \Phi) dt \leq \frac{1}{\rho} \left(\xi(t_0) + W \cdot \int_{t_0}^{+\infty} \Gamma(t)\|g(t)\| dt \right) < +\infty. \quad (5.18)$$

Therefore, the second conclusion in Theorem 5.1 holds.

Thus ends the proof. \square

6. Comparison of first-order and second-order gradient dynamical systems

Next, the first-order dynamical system method, the second-order dynamical system method without external action, and the second-order dynamical system method based on external action proposed in this paper are compared theoretically; the results are summarized in Table 1.

In the Table 1, I refers to the first-order dynamical system, II refers to the second-order dynamical system without external action, and III refers to the second-order dynamical system based on external action.

From Table 1, we can see that the conditions for the first-order dynamical system are quite stringent, whereas the conditions for the second-order dynamical system are more relaxed, but the objective function needs to be convex. Therefore, the second-order dynamical system is preferred when solving optimization problems with convex objective functions.

Table 1. Comparison of solution conditions for three dynamical systems.

Conditions	I	II	III
The convexity of Φ		✓	✓
$\operatorname{argmin} \Phi \neq \emptyset$	✓	✓	✓
The compact of $\operatorname{argmin} \Phi$	✓		
The non-singularity of $\nabla\Phi$	✓		

7. Numerical simulation analysis

In this section, in order to determine more intuitively the feasibility and validity of the second-order dynamical system method constructed in this paper, we determine whether the presence or absence of external perturbations will have an effect on the second-order dynamical system. On the basis of employing the control-variable method, we conducted numerical simulation experiments on the first-order dynamical system (4.2), the second-order dynamical system (4.3), and the second-order dynamical system with disturbances (5.1). All numerical experiments were conducted in the MATLAB R2023a computational environment. Based on our prior research experience, the relevant parameters of the dynamical system in this paper were randomly selected as follows: the scaling factor of the first-order dynamical system (4.2) was taken as $\rho = 100$, and the viscous damping parameter of the second-order dynamical system was taken as $\alpha = 25$.

In order to verify the advantages of the parameter $\beta(t)$ in the proposed dynamical system, the first three numerical cases were conducted at the standard time scale $\beta(t) = 1$. The fourth numerical experiment used constant $\beta(t)$ and nonconstant $\beta(t) = 2t$ for comparison in order to verify that the introduction of the nonconstant parameter $\beta(t)$ in this paper is superior to the constant parameter $\beta(t) = 1$ in terms of convergence speed.

Example I: Consider the following optimization problem:

$$\begin{aligned} \min f_1(x) &= 15 - x_1^2 - x_2^2 \\ \text{s.t. } (x_1 + 1)\text{sgn}(x_1 - 1) \frac{\sqrt{1 + 10000(x_1 - 1)^2}}{100} + \frac{2}{5}x_2^2 - 1 &\leq 0, \\ \frac{\sqrt{1 + 10000(x_2 - x_1 + 1)^2}}{100} \text{sgn}(x_2 - x_1 + 1) &\leq 0, \\ -x_2 &\leq 0. \end{aligned} \quad (7.1)$$

First, the sign function is approximated and replaced using the smooth function $\psi(k_i(x), a) = ak_i(x) / \sqrt{1 + (ak_i(x))^2}$ with $a = 100$. Consequently, it can be derived that:

$$\begin{aligned} \min f(x) &= 15 - x_1^2 - x_2^2 \\ \text{s.t. } x_1^2 + \frac{2}{5}x_2^2 - 2 &\leq 0, \\ -x_1 + x_2 + 1 &\leq 0, \\ -x_2 &\leq 0. \end{aligned} \quad (7.2)$$

This is then transformed into an unconstrained optimization problem using the penalty function method in the following mathematical form:

$$\min \Phi(x, r_k) = 15 - x_1^2 - x_2^2 + r_k \left(\sum_{i=1}^3 \{\max(0, g_i(x))\}^2 \right), \quad (7.3)$$

where $g_1(x) = x_1^2 + 2x_2^2/5 - 2$, $g_2(x) = -x_1 + x_2 + 1$, and $g_3(x) = -x_2$. The penalty parameter was taken as $r_k = 10^6$.

Next, we solve the problem (7.3) using first-order dynamic systems and the two forms of second-order dynamic systems established in this paper.

1) Using the first-order dynamic system method (4.2) for the solution, the simulation results are shown in Figures 3 and 4:

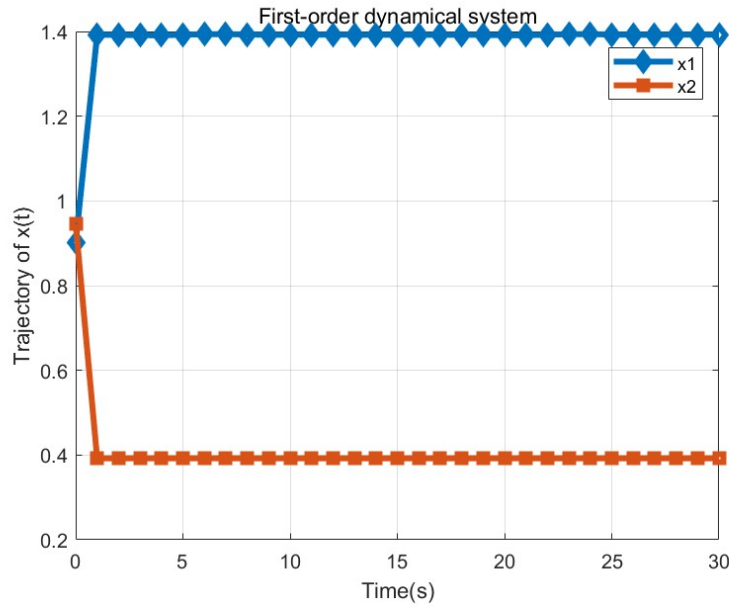


Figure 3. Trajectory of the solution $x(t)$ for first-order dynamic system (4.2).

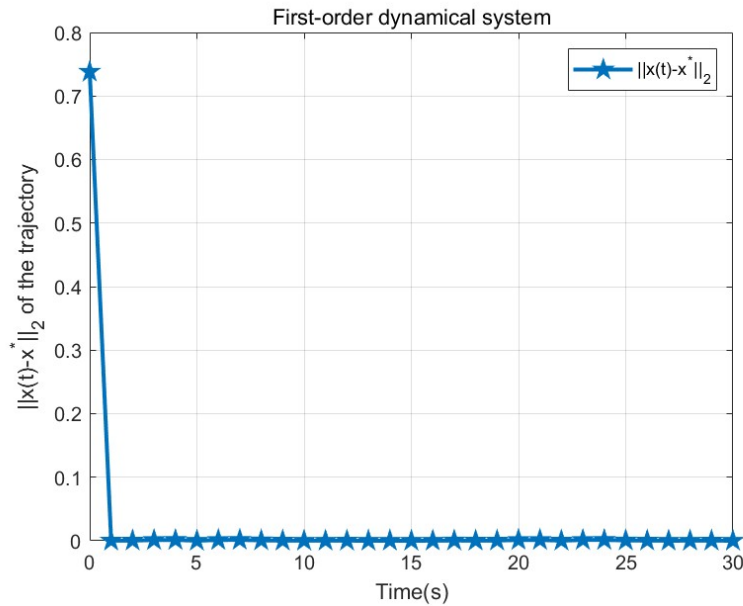


Figure 4. Error rate of $\|x(t) - x^*\|_2$ for first-order dynamic system (4.2).

2) Using the first form of the second-order dynamic system method (4.3) for the solution, the simulation

results are shown in Figures 5 and 6:

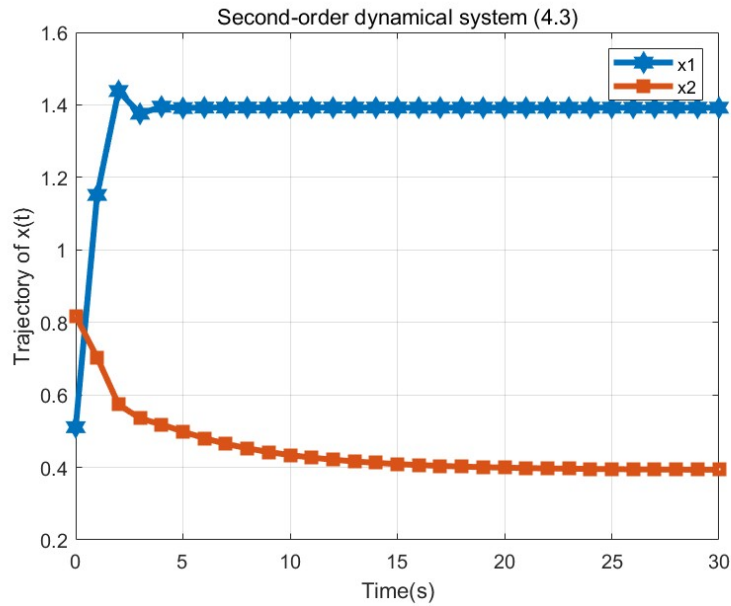


Figure 5. Trajectory of the solution $x(t)$ for second-order dynamic system (4.3).

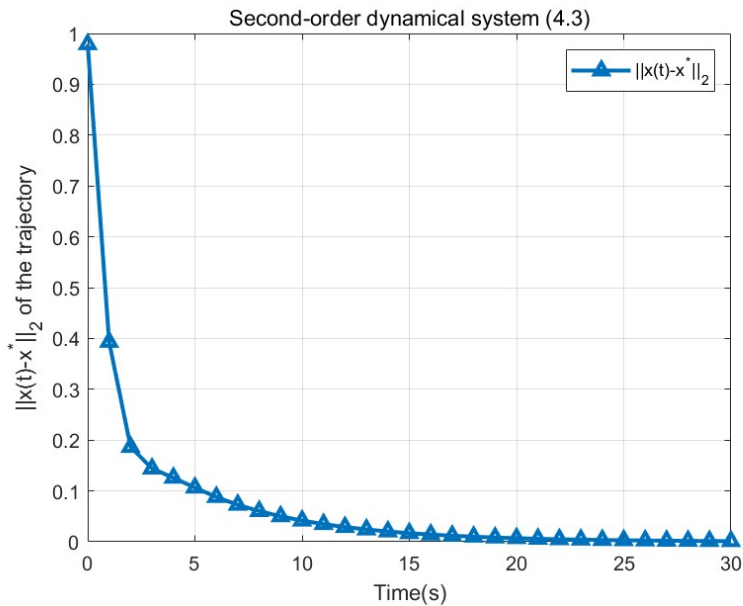


Figure 6. Error rate of $\|x(t) - x^*\|_2$ for second-order dynamic system (4.3).

3) To determine whether external disturbances affect second-order dynamical systems, we employed the second formulation of the second-order dynamical system method (5.1) for the solution with an external disturbance $g(t) = 0.00001$. The simulation results are shown in Figures 7 and 8:

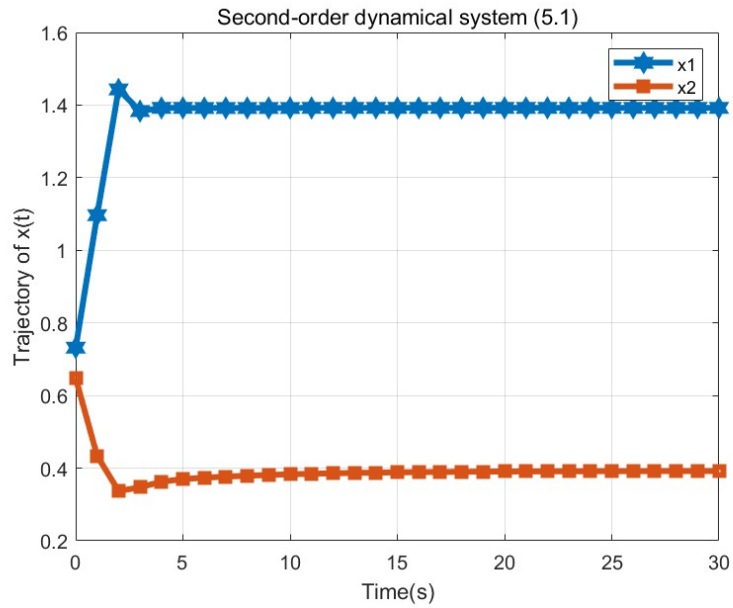


Figure 7. Trajectory of the solution $x(t)$ under external action $g(t) = 0.00001$.

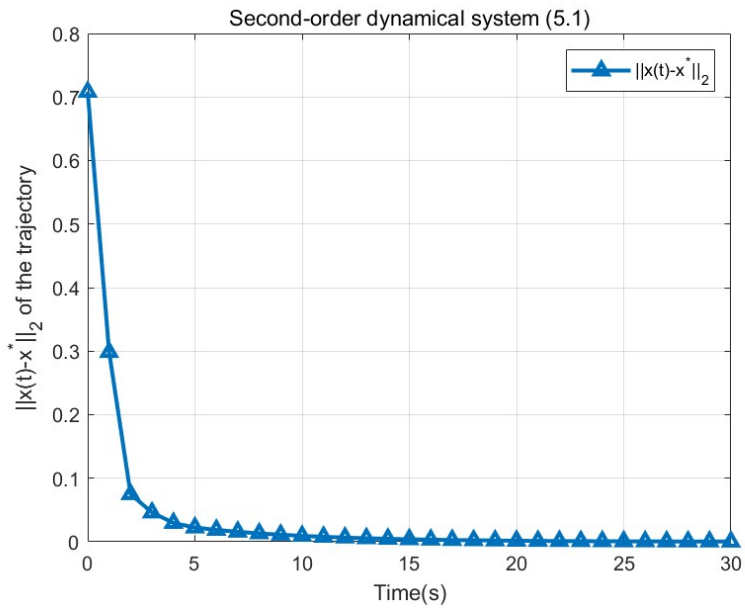


Figure 8. Error rate of $\|x(t) - x^*\|_2$ under external action $g(t) = 0.00001$.

In light of the results depicted from Figure 3 to Figure 8, it can be concluded that both the first-order and second-order dynamical systems are capable of driving the solution toward the optimal point. The second-order systems show different convergence behaviors compared to the first-order one, and they also exhibit a certain level of robustness when subjected to small external disturbances.

Table 2 illustrates the CPU runtime required to meet the termination condition, demonstrating that the two forms of second-order dynamic systems exhibit similar efficiency, whereas the first-order

dynamic system shows the lowest efficiency.

Table 2. The CPU time required for the three dynamical systems in Problem I to reach the termination condition.

Optimization Algorithm	System (4.2)	System (4.3)	System (5.1)
Operating Time(s)	0.053421	0.013681	0.011929

The solutions to this problem are $x_1 = 1.3923$ and $x_2 = 0.3923$. As shown in Table 3, the solutions from all three dynamical systems converge to the solution of the optimization problem. Despite their structural differences (first-order versus second-order), the numerical solutions generated by these three systems for Problem I are nearly identical.

Table 3. A comparison of numerical results for Problem I obtained using first-order dynamical systems (4.2) and second-order dynamical systems (4.3) and (5.1).

Optimization Algorithm	System (4.2)	System (4.3)	System (5.1)
Experiment Results	$\begin{pmatrix} 1.3924 \\ 0.3923 \end{pmatrix}$	$\begin{pmatrix} 1.3923 \\ 0.3923 \end{pmatrix}$	$\begin{pmatrix} 1.3923 \\ 0.3923 \end{pmatrix}$

Example II: Consider the following optimization problem:

$$\begin{aligned}
 \min f_2(x) &= x_1^2 + x_2^2 + x_3^2 \\
 \text{s.t. } (x_1 + 2x_2)\text{sgn}(x_1 - x_2) &\leq 1, \\
 (2 - x_2)\text{sgn}(x_3 - 1) &\leq 2, \\
 \text{sgn}(x_1^2 - x_3) &\leq 3.
 \end{aligned} \tag{7.4}$$

It is approximated using the smooth function $\psi(k_i(x), 100) = 100k_i(x) / \sqrt{1 + (100k_i(x))^2}$, which can be obtained by the following:

$$\begin{aligned}
 \min f_2(x) &= x_1^2 + x_2^2 + x_3^2 \\
 \text{s.t. } (x_1 + 2x_2) \frac{100(x_1 - x_2)}{\sqrt{1 + (100(x_1 - x_2))^2}} &\leq 1, \\
 (2 - x_2) \frac{100(x_3 - 1)}{\sqrt{1 + (100(x_3 - 1))^2}} &\leq 2, \\
 \frac{100(x_1^2 - x_3)}{\sqrt{1 + (100(x_1^2 - x_3))^2}} &\leq 3.
 \end{aligned} \tag{7.5}$$

This is then transformed into an unconstrained optimization problem using the penalty function method in the following mathematical form:

$$\min \Phi(x, r_k) = x_1^2 + x_2^2 + x_3^2 + r_k \left(\sum_{i=1}^3 \{\max(0, g_i(x))\}^2 \right), \tag{7.6}$$

where we take $r_k = 10^6$, and

$$\begin{cases} g_1(x) = (x_1 + 2x_2) \frac{100(x_1 - x_2)}{\sqrt{1 + (100(x_1 - x_2))^2}} - 1, \\ g_2(x) = (2 - x_2) \frac{100(x_3 - 1)}{\sqrt{1 + (100(x_3 - 1))^2}} - 2, \\ g_3(x) = \frac{100(x_1^2 - x_3)}{\sqrt{1 + (100(x_1^2 - x_3))^2}} - 3. \end{cases}$$

Next, we solve the problem (7.6) using first-order dynamic systems and the two forms of second-order dynamic systems established in this paper.

1) Figures 9 and 10 present the numerical results obtained by solving the optimization problem (7.6) using the first-order dynamical system (4.2):

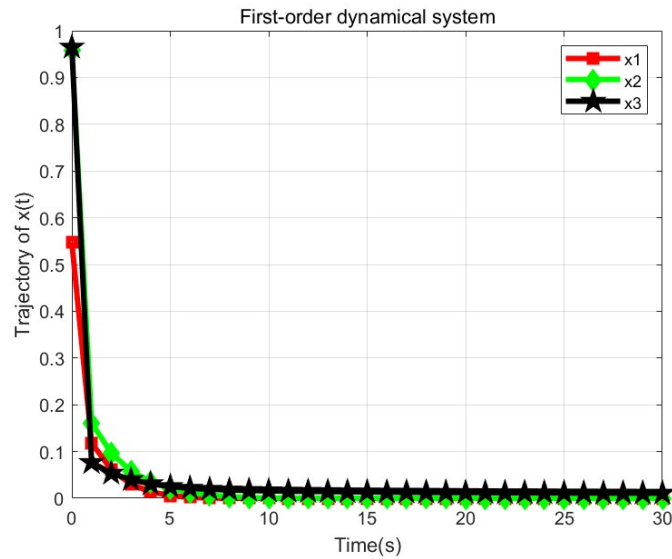


Figure 9. Trajectory of the solution $x(t)$ for first-order system (4.2).

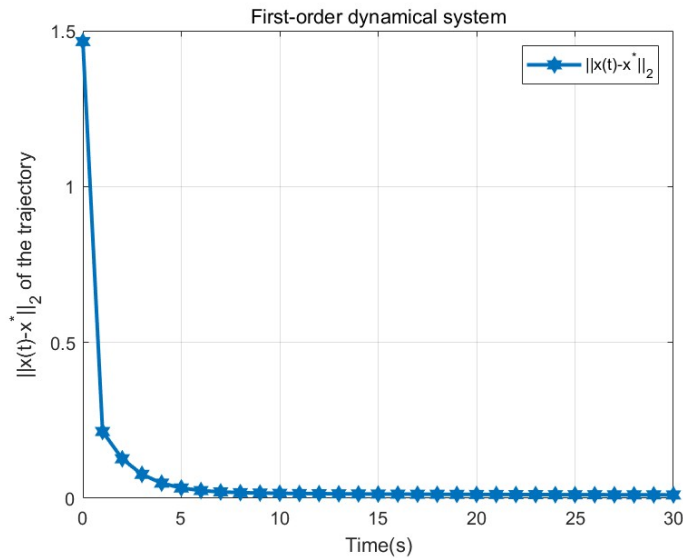


Figure 10. Error rate of $\|x(t) - x^*\|_2$ for first-order system (4.2).

2) Using the first form of the second-order dynamic system method (4.3) for the solution, the numerical results of solving the optimization problem (7.6) for the undisturbed second-order dynamical system (4.3) are shown in Figures 11 and 12 below:

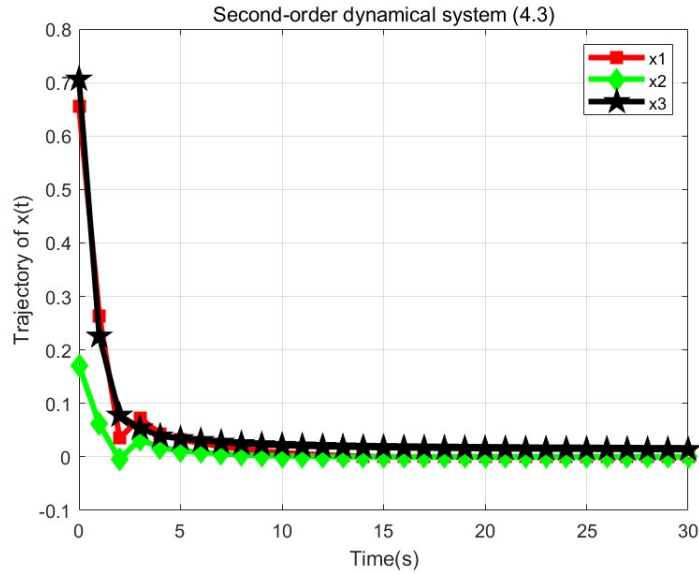


Figure 11. Trajectory of the solution $x(t)$ for second-order system (4.3).

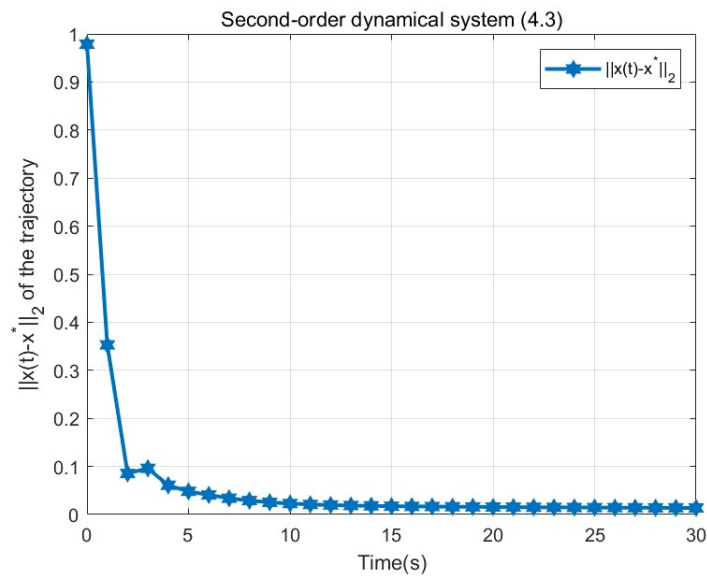


Figure 12. Error rate of $\|x(t) - x^*\|_2$ for second-order system (4.3).

3) To determine whether external disturbances affect second-order dynamical systems under the same preconditions, the solution is performed using the second-order dynamical system method (5.1) based on the external perturbation under which $g(t) = 0.00001$. The simulation results are shown in Figures 13 and 14:

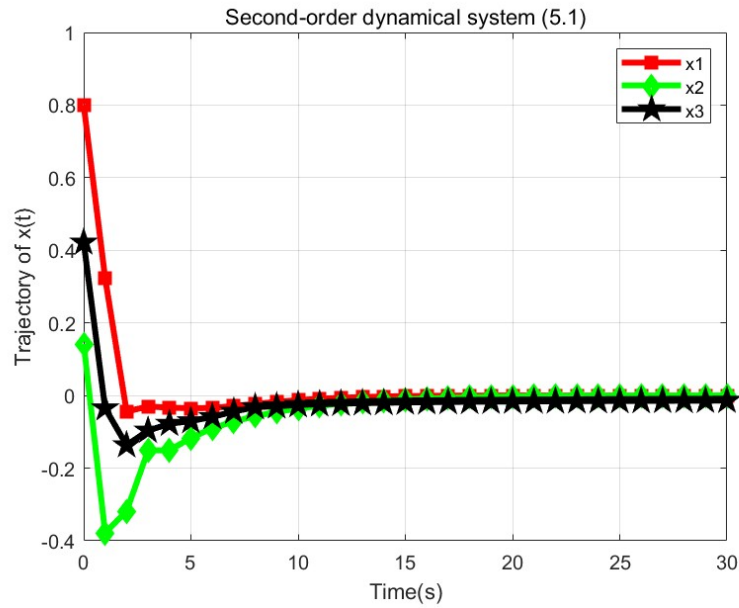


Figure 13. Trajectory of the solution $x(t)$ under external action.

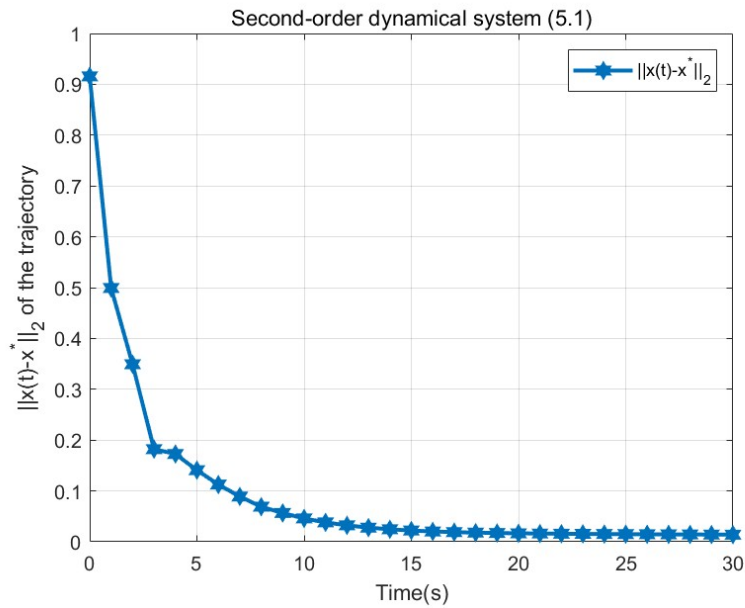


Figure 14. Error rate of $\|x(t) - x^*\|_2$ under external action.

In light of the results depicted from Figure 9 to Figure 14, it can be concluded that both the first-order and second-order dynamical systems are capable of driving the solution towards the optimal point. The second-order systems show different convergence behaviors compared to the first-order one, and they also exhibit a certain level of robustness when subjected to small external disturbances.

Table 4 illustrates the CPU runtime required to meet the termination condition, demonstrating that the two forms of second-order dynamic systems exhibit similar efficiency, whereas the first-order

dynamic system shows the lowest efficiency.

Table 4. The CPU time required for the three dynamical systems in Problem II to reach the termination condition.

Optimization Algorithm	System (4.2)	System (4.3)	System (5.1)
Operating Time(s)	0.298994	0.119787	0.134705

The solution to this problem is $x = [0, 0, 0]^T$. As shown in Table 5, the solutions from all three dynamical systems converge to the solution of the optimization problem. Despite their structural differences (first-order versus second-order), the numerical solutions generated by these three systems for Problem II are nearly identical.

Table 5. A comparison of numerical results for Problem II obtained using first-order dynamical systems (4.2) and second-order dynamical systems (4.3) and (5.1).

Optimization Algorithm	System (4.2)	System (4.3)	System (5.1)
Experiment Results	$\begin{pmatrix} 6.9290 \times 10^{-32} \\ 2.7090 \times 10^{-09} \\ 0.0108 \end{pmatrix}$	$\begin{pmatrix} 2.3641 \times 10^{-06} \\ 1.5113 \times 10^{-06} \\ 0.0138 \end{pmatrix}$	$\begin{pmatrix} 2.6083 \times 10^{-06} \\ -9.7427 \times 10^{-05} \\ -0.0141 \end{pmatrix}$

Example III: Consider the following optimization problem:

$$\begin{aligned}
 \min f_2(x) &= 5x_1^2 + 13x_2^2 + x_3^2 - 2x_1x_2 + 2x_1x_3 + 6x_2x_3 \\
 \text{s.t. } x_1^3 - 6x_2 - \frac{\text{sgn}(x_3)}{5} \sqrt{1 + (20x_3)^2} &\leq 0, \\
 x_1 + x_2 + x_3 &= 1, \\
 x_1 &\leq 0.
 \end{aligned} \tag{7.7}$$

To begin, using the smooth function $\psi(k_i(x), 20) = 20k_i(x)/\sqrt{1 + (20k_i(x))^2}$ for approximation, we can obtain:

$$\begin{aligned}
 \min f_2(x) &= 5x_1^2 + 13x_2^2 + x_3^2 - 2x_1x_2 + 2x_1x_3 + 6x_2x_3 \\
 \text{s.t. } x_1^3 - 6x_2 - 4x_3 &\leq 0, \\
 x_1 + x_2 + x_3 &= 1, \\
 x_1 &\leq 0.
 \end{aligned} \tag{7.8}$$

Then, use the penalty function method to transform it into an unconstrained optimization problem and then solve it using the methods proposed above.

The optimal solution to this problem is $x = [-0.5, -0.5, 2]^T$. From Figures 15–17, it can be seen that the solution of the second-order dynamical system converges to the solution of the original problem with or without external disturbances. However, from Table 6, it can be seen that compared to first-order dynamical systems, second-order dynamical systems have shorter operating times and faster convergence speeds.

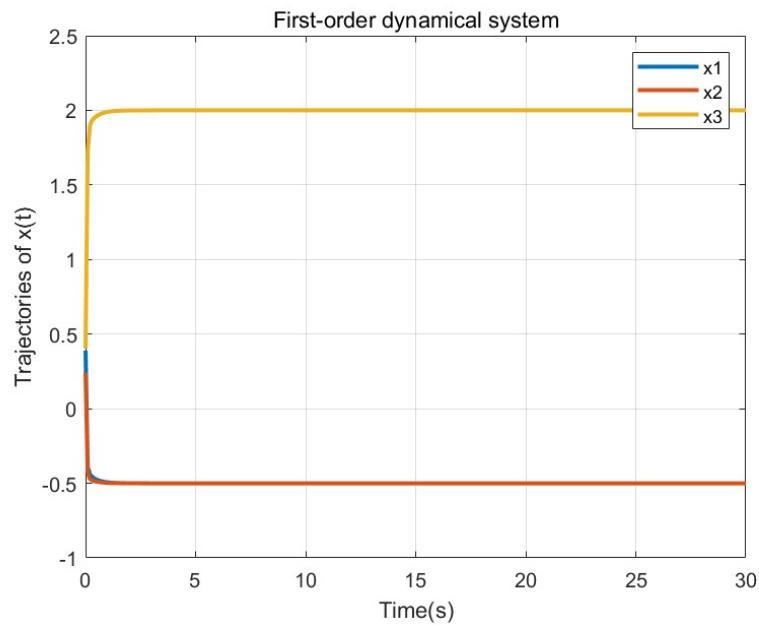


Figure 15. First-order system (4.2).

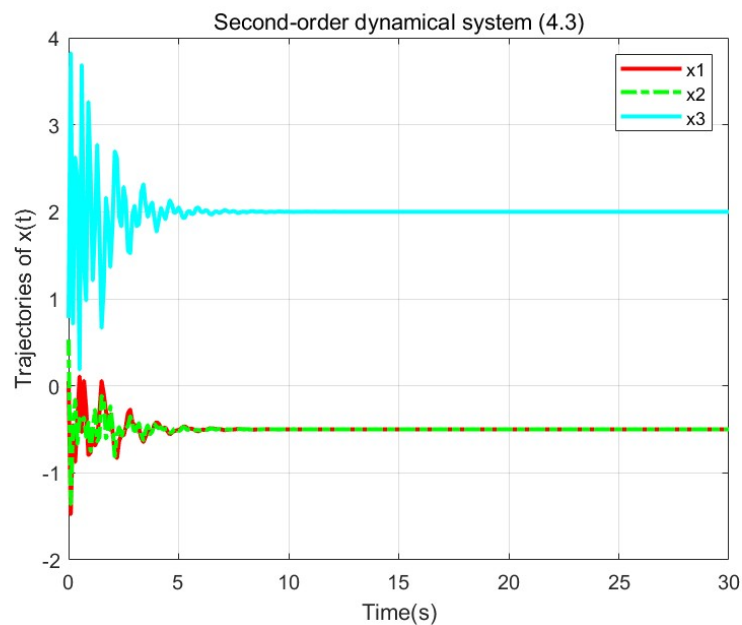


Figure 16. Second-order system (4.3).

To further verify whether the two methods proposed in this article for solving Example III will depend on the selection of initial points, we selected three randomly chosen initial points: $X_1 = [0.5, 1, 0.5]^T$, $X_2 = [1.0, 0.5, -1]^T$, and $X_3 = [1.5, 2.5, 0]^T$. The simulation results are shown in Figures 18 and 19.

From Figures 18 and 19, it can be seen that even with different initial point selections, the second-

order dynamical systems (4.3) and (5.1) can converge to the optimal solution of the original problem.

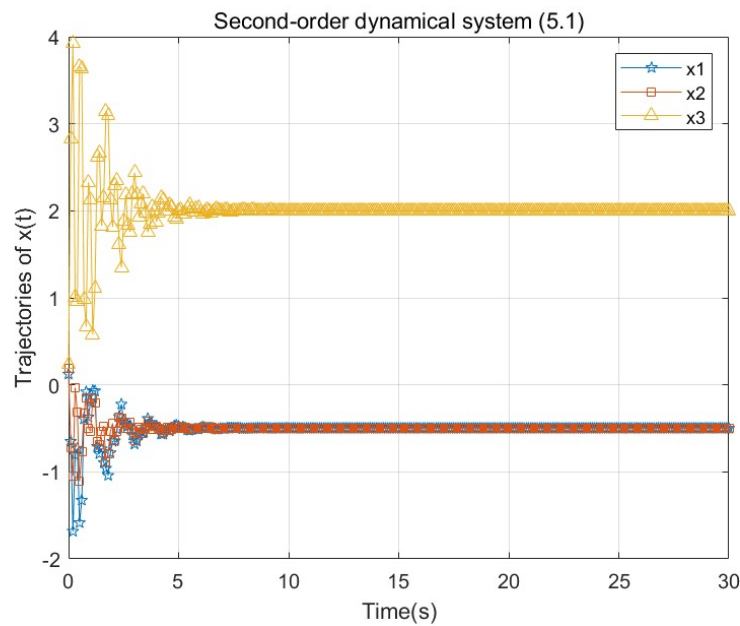


Figure 17. Second-order system (5.1).

Table 6. A comparison of numerical results for Problem III obtained using first-order dynamical systems (4.2) and second-order dynamical systems (4.3) and (5.1).

Optimization Algorithm	System (4.2)	System (4.3)	System (5.1)
Experiment Results	$\begin{pmatrix} -0.5 \\ -0.5 \\ 2.0 \end{pmatrix}$	$\begin{pmatrix} -0.5 \\ -0.5 \\ 2.0 \end{pmatrix}$	$\begin{pmatrix} -0.5 \\ -0.5 \\ 2.0 \end{pmatrix}$
Operating Time(s)	5.219891	4.924299	4.903694

The above three examples are all based on the standard time scale $\beta(t) = 1$. In order to further verify the advantages brought by the dynamically changing time scale parameter $\beta(t)$ to the dynamic system methods (4.3) and (5.1), Example IV is given below, and simulation experiments are conducted using fixed $\beta(t) = 1$ and dynamically changing $\beta(t) = O(t) = 2t$ for comparison.

Example IV: Consider the following optimization problem:

$$\begin{aligned}
 \min f_4(x) &= x_1^2 + 2x_2^2 + 2x_1x_2 - 10x_1 - 12x_2 \\
 \text{s.t. } &\sqrt{1 + (20\text{sgn}(x_1 + 3x_2 - 8))^2} \text{sgn}(x_1 + 3x_2 - 8) \leq 0, \\
 &x_1^2 + x_2^2 + 2x_1 - 2x_2 - 3 \leq 0.
 \end{aligned} \tag{7.9}$$

First, using the smooth function $\psi(k_i(x), 20) = 20k_i(x)/\sqrt{1 + (20k_i(x))^2}$ for approximation, we can obtain

$$\begin{aligned}
 \min f_4(x) &= x_1^2 + 2x_2^2 + 2x_1x_2 - 10x_1 - 12x_2 \\
 \text{s.t. } &20(x_1 + 3x_2 - 8) \leq 0, \\
 &x_1^2 + x_2^2 + 2x_1 - 2x_2 - 3 \leq 0.
 \end{aligned} \tag{7.10}$$

Then, we use the penalty function method to transform it into an unconstrained optimization problem. Next, under the two conditions $\beta(t) = 1$ and $\beta(t) = O(t) = 2t$, the dynamic system (4.3) is used for solving, and the simulation results are obtained.

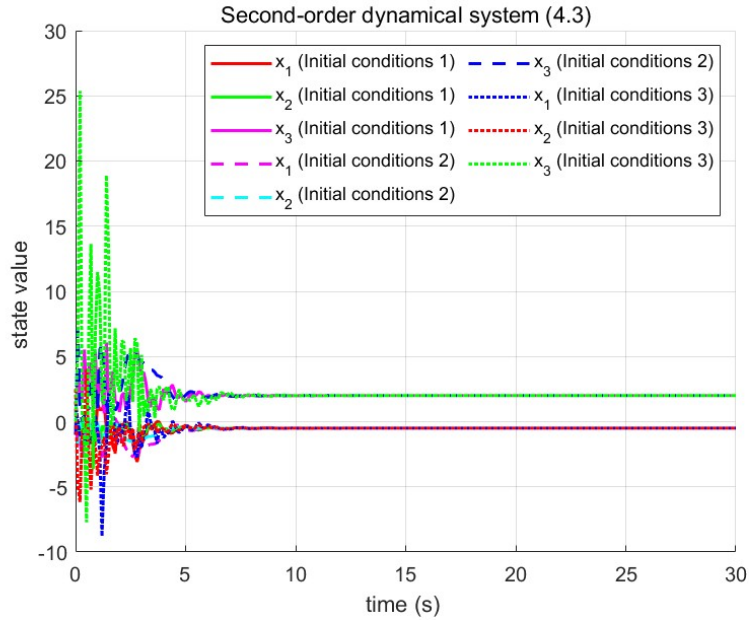


Figure 18. Trajectory diagram of second-order system (4.3) under different initial points.

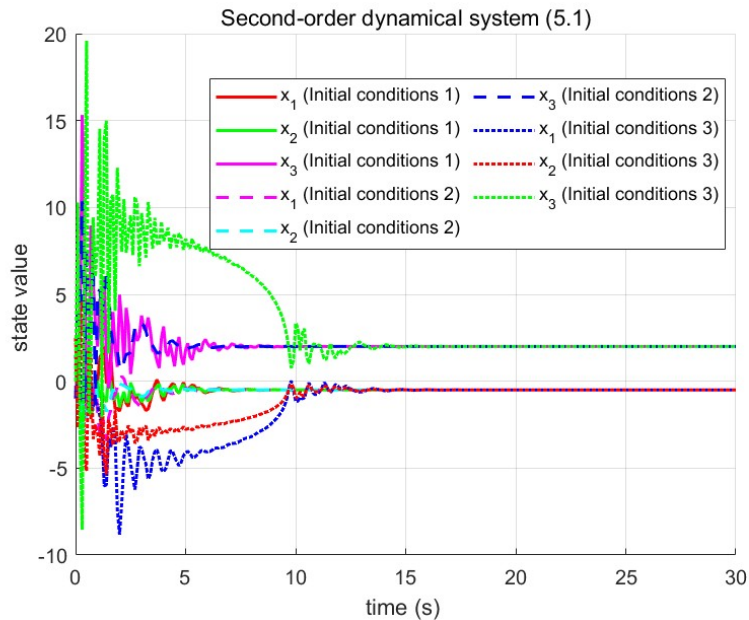


Figure 19. Trajectory diagram of second-order system (5.1) under different initial points.

For the undisturbed dynamical system (4.3), through the comparison of simulation experiments in

Figures 20 and 21 as well as Figures 22 and 23, it was found that the nonconstant parameter $\beta(t)$ converges faster and has a stronger effect than the constant parameter $\beta(t) = 1$. This further indicates that the introduction of the dynamic parameter $\beta(t)$ in this paper can promote the solving speed of the undisturbed dynamical system (4.3).

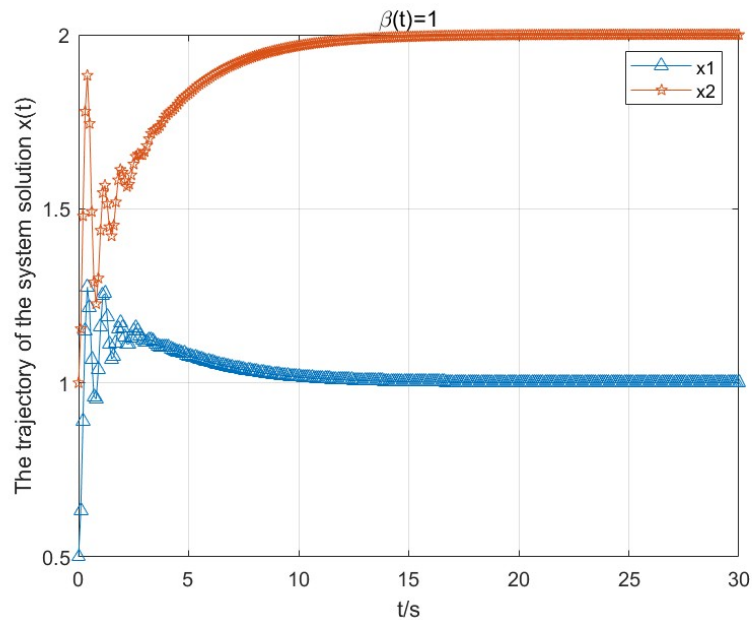


Figure 20. State solution trajectory diagram of second-order system (4.3) based on $\beta(t) = 1$.

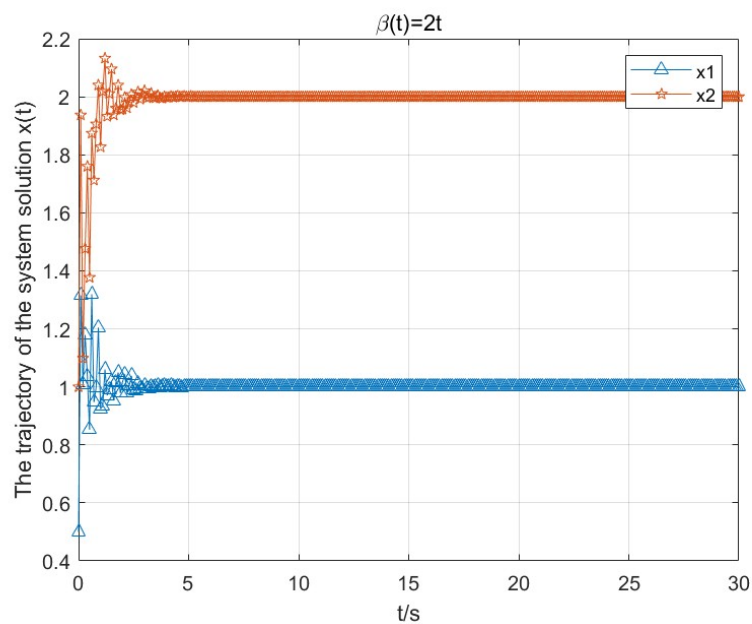


Figure 21. State solution trajectory diagram of second-order system (4.3) based on $\beta(t) = 2t$.

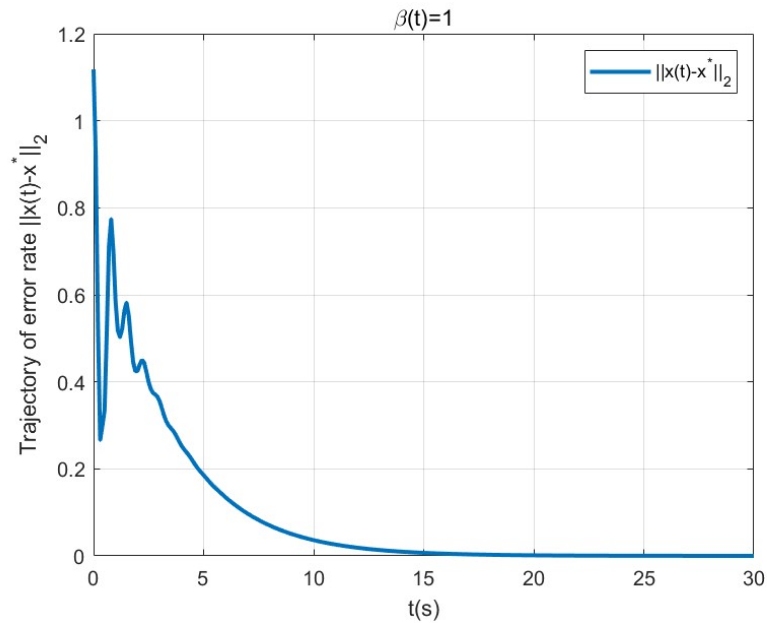


Figure 22. Error rate trajectory diagram of second-order system (4.3) based on $\beta(t) = 1$.

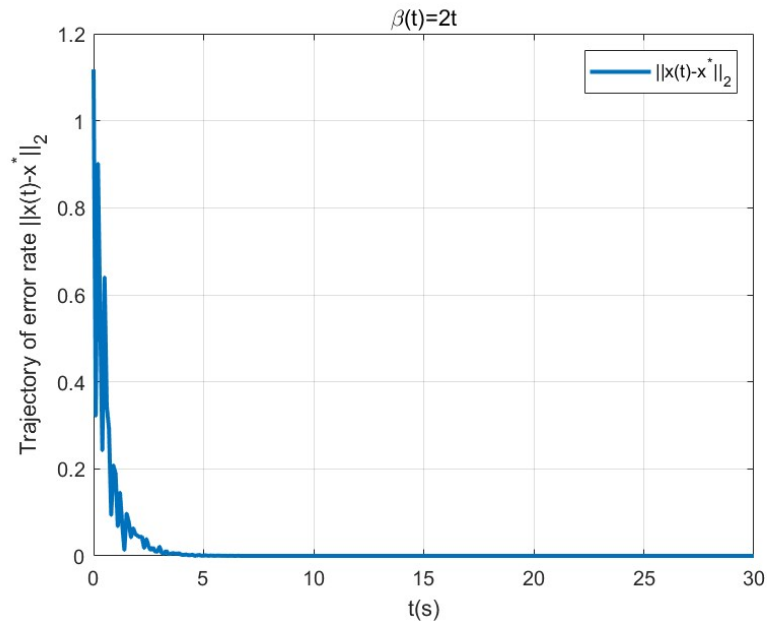


Figure 23. Error rate trajectory diagram of second-order system (4.3) based on $\beta(t) = 2t$.

Finally, under conditions $\beta(t) = 1$ and $\beta(t) = O(t) = 2t$, the dynamic system (5.1) was used for solving, and the simulation results were obtained.

Regarding the disturbance dynamic system (5.1), through the comparison of simulation experiments in Figures 24 and 25 as well as Figures 26 and 27, it was found that the nonconstant parameter $\beta(t)$ converges faster and has a stronger effect than the constant parameter $\beta(t) = 1$. This further indicates

that the introduction of the dynamic parameter $\beta(t)$ in this paper can promote the solving speed of the dynamic system (5.1) under disturbance.

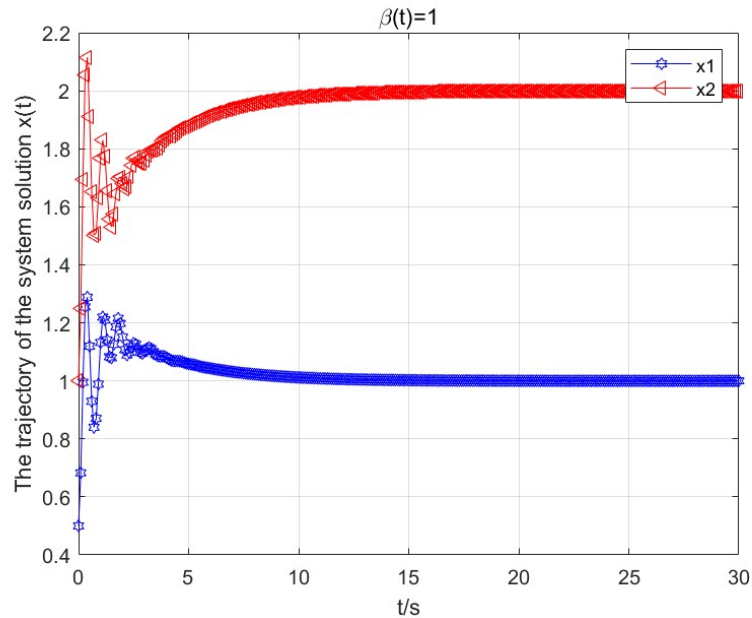


Figure 24. State solution trajectory diagram of second-order system (5.1) based on $\beta(t) = 1$.

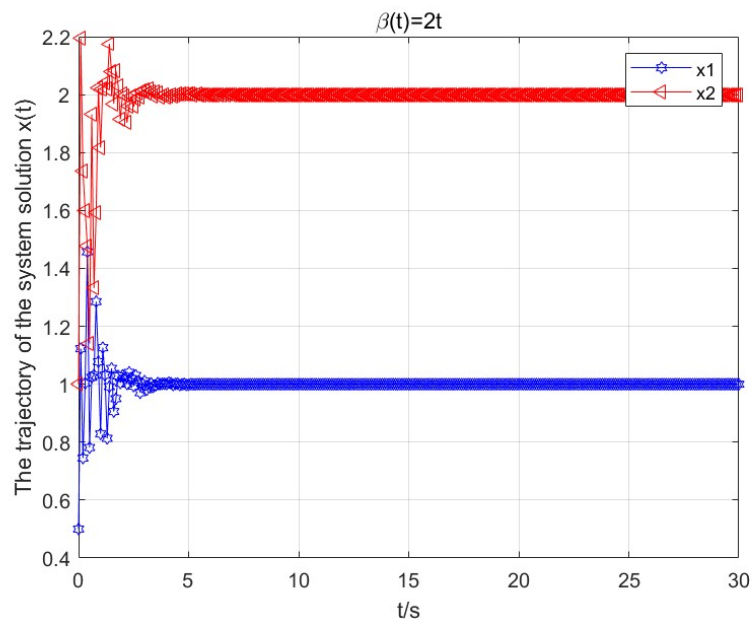


Figure 25. State solution trajectory diagram of second-order system (5.1) based on $\beta(t) = 2t$.

Combining the simulation results of the above four numerical examples, it can be seen that the trajectories of the solutions of the second-order dynamical system always all converge to the optimal

solution of the original optimization problem with or without the presence of external perturbations, thus verifying the effectiveness of the dynamical system. Further, the introduced dynamic parameter $\beta(t)$ can improve the convergence ability and problem-solving speed of the dynamical system compared to the static parameter $\beta(t) = 1$.

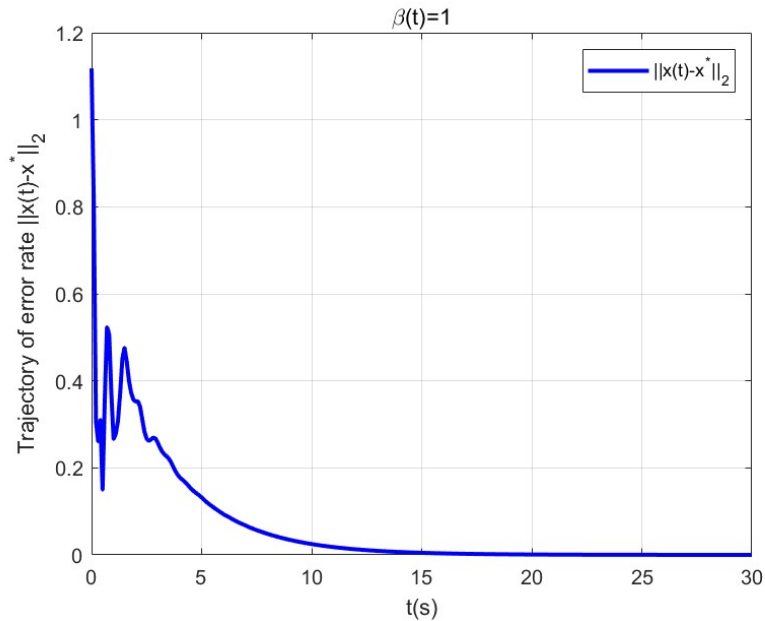


Figure 26. Error rate trajectory diagram of second-order system (5.1) based on $\beta(t) = 1$.

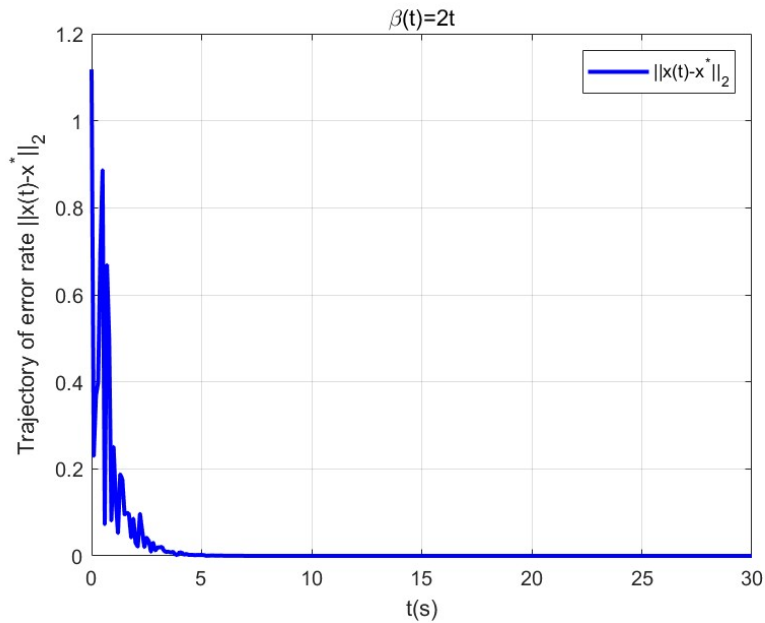


Figure 27. Error rate trajectory diagram of second-order system (5.1) based on $\beta(t) = 2t$.

8. Conclusions

This paper conducts an in-depth investigation into a class of nonlinear optimization problems which hold significant theoretical importance and have extensive engineering applications.

First, based on relevant mathematical optimization theories, this paper proposes an innovative smoothing approach that transforms the original optimization problem model into a differentiable optimization problem model. Second, building upon this foundation, the penalty function method is adopted. By introducing penalty parameter factors, an exact penalty function is formulated to establish an equivalent unconstrained optimization problem. Subsequently, drawing inspiration from first-order dynamical systems, this paper proposes two forms of second-order dynamical systems: one without perturbation and the other with perturbation, aimed at solving the aforementioned unconstrained optimization problem. Moreover, through Lyapunov analysis, positive energy functions are constructed to separately analyze their global convergence. Finally, for the two forms of second-order dynamical systems, the control variable method was employed to select identical parameters, and relevant numerical experiments were conducted. The results demonstrate that both forms of the dynamical systems exhibit good feasibility and effectiveness. Moreover, the presence or absence of external perturbations has little to no impact on the constructed second-order dynamical systems.

It is noteworthy that research focused on solving this specific category of nonlinear optimization problems through the dynamical system approach remains at a nascent stage. In the realms of theoretical analysis and algorithm design, numerous scientific challenges persist and await resolution. This situation thus delineates a crucial avenue for subsequent research endeavors.

Use of AI tools declaration

The authors declare they have not used Artificial Intelligence (AI) tools in the creation of this article.

Acknowledgments

This study was supported by the National Natural Science Foundation of China (Project No. 52475482).

Conflict of interest

The authors declare no conflict of interest.

References

1. A. Bensoussan, J. Lions, Optimal impulse and continuous control: Method of non linear quasi-variational inequalities, *Trudy Mat. Inst. Steklov*, **134** (1975), 5–22.
2. W. Gong, Y. Ho, Smoothed (conditional) perturbation analysis of discrete event dynamical systems, *IEEE Trans. Autom. Control*, **32** (1987), 858–866. <http://doi.org/10.1109/TAC.1987.1104464>

3. R. Rubinstein, How to optimize discrete-event systems from a single sample path by the score function method, *Ann. Oper. Res.*, **27** (1990), 175–212. <https://doi.org/10.1007/BF02055195>
4. J. Zhang, L. Zhao, A class of optimization problems with discontinuous constraints and applications, *J. Xiamen Univ. Nat. Sci.*, **49** (2010), 16–19.
5. A. M. Gupal, V. I. Norkin, Algorithm for the minimization of discontinuous functions, *Cybernetics*, **13** (1977), 220–223. <http://doi.org/10.1007/BF01073313>
6. Y. Ermoliev, V. Norkin, On constrained discontinuous optimization, in *Stochastic Programming Methods and Technical Applications*, **458** (1998), 128–144. https://doi.org/10.1007/978-3-642-45767-8_7
7. V. Y. Katkovnik, O. Y. Kul'chitskii, Convergence of one class of random search algorithms, *Autom. Remote Control*, **33** (1972), 1321–1326.
8. J. Warga, Necessary conditions without differentiability assumptions in optimal control, *J. Differ. Equations*, **18** (1975), 41–62. [http://doi.org/10.1016/0022-0396\(75\)90080-7](http://doi.org/10.1016/0022-0396(75)90080-7)
9. V. D. Batukhtin, An approach to the solution of discontinuous extremal problems, *J. Comput. Syst. Sci. Int.*, **33** (1995), 30–38.
10. Y. M. Ermoliev, V. I. Norkin, R. J. Wets, The minimization of semicontinuous functions: mollifier subgradients, *SIAM J. Control Optim.*, **33** (1995), 149–167. <http://doi.org/10.1137/S0363012992238369>
11. H. T. Jongen, O. Stein, Smoothing by mollifiers. Part I: Semi-infinite optimization, *J. Glob. Optim.*, **41** (2008), 319–334. <http://doi.org/10.1007/s10898-007-9232-3>
12. H. T. Jongen, O. Stein, Smoothing by mollifiers. Part II: Nonlinear optimization, *J. Glob. Optim.*, **41** (2008), 335–350. <http://doi.org/10.1007/s10898-007-9231-4>
13. Y. Cui, J. Liu, J. Pang, The minimization of piecewise functions: Pseudo stationarity, preprint, arXiv:2305.14798.
14. B. W. Kort, D. P. Bertsekas, A new penalty function method for constrained minimization, in *Proceedings of the 1972 IEEE Conference on Decision and Control and 11th Symposium on Adaptive Processes*, (1972), 162–166. <http://doi.org/10.1109/CDC.1972.268971>
15. Ö. Yeniay, Penalty function methods for constrained optimization with genetic algorithms, *Math. Comput. Appl.*, **10** (2005), 45–56. <http://doi.org/10.3390/mca10010045>
16. Q. Wu, *A Bundle Methods for A Class of Nonconvex and Nonsmooth Optimization Problems and Applications*, Ph.D. Thesis, Dalian University of Technology in Dalian, 2022. <http://doi.org/10.26991/d.cnki.gdllu.2021.003891>
17. J. Sun, W. Fu, J. H. Alcantara, J. Chen, A neural network based on the metric projector for solving soccvi problem, *IEEE Trans. Neural Networks Learn. Syst.*, **32** (2021), 2886–2900. <http://doi.org/10.1109/TNNLS.2020.3008661>
18. H. Attouch, J. Peypouquet, P. Redont, Fast convex optimization via inertial dynamics with hessian driven damping, *J. Differ. Equations*, **261** (2016), 5734–5783. <http://doi.org/10.1016/j.jde.2016.08.020>
19. H. Attouch, Z. Chbani, H. Riahi, Fast convex optimization via time scaling of damped inertial gradient dynamics, 2019. Available from: <https://hal.science/hal-02138954>.

-
20. A. Cabot, H. Engler, S. Gadat, On the long time behavior of second order differential equations with asymptotically small dissipation, *Trans. Am. Math. Soc.*, **361** (2009), 5983–6017. <http://doi.org/10.1090/S0002-9947-09-04785-0>
21. A. Cabot, P. Frankel, Asymptotics for some semilinear hyperbolic equations with non-autonomous damping, *J. Differ. Equations*, **252** (2012), 294–322. <http://doi.org/10.1016/j.jde.2011.09.012>



AIMS Press

© 2026 the Author(s), licensee AIMS Press. This is an open access article distributed under the terms of the Creative Commons Attribution License (<https://creativecommons.org/licenses/by/4.0>)